# Evaluation of the Propagation Characteristics of Ultra-Wideband Communication Channels*

ROBERT A. SCHOLTZ, FELLOW, IEEE
R. JEAN-MARC CRAMER, MEMBER, IEEE
MOE Z. WIN, SENIOR MEMBER, IEEE

February 4, 1998

**ABSTRACT**

**A novel application of the CLEAN algorithm is proposed to characterize ultra-wideband (UWB) communication channels from measured data.**

## I. Introduction

In order to gain a more complete understanding of the potential of ultra-wide-band (UWB) radio communication systems, it is important to have an accurate model of the propagation characteristics of the transmitted waveforms. In particular, the existence of multipath components arriving at the receiver with different time delays and from different directions can create a dynamic and extended channel impulse response. Characterization of the propagation channel may therefore influence the design of RAKE receiver diversity algorithms for this channel. This paper presents a technique for the analysis of UWB signals received on an array of sensors. The goal is to use this technique to develop channel models on which spatio-temporal UWB radio algorithms can be tested with confidence. Implicit in this is an understanding of the distortions experienced along individual propagation paths.

A definition for UWB signals is given in [6] as those whose fractional bandwidth is greater than 25%. A number of different signals satisfy this constraint, including the Gaussian pulse and its derivatives employed in this work.

### A. Impulse Radio Fundamentals

The theoretical performance of UWB impulse radio communication systems has been investigated in the absence of degradations due to multipath interference [1], [2], [3]. The information bearing signal associated with impulse radio is a time-hopped, pulse-position modulated signal, with many pulses used to represent one data symbol. Both multiple-access addressing via distinct hopping patterns and information are encoded in time-shifts relative to the frame clock.

The ideally modeled pulse shape propagating in free space is the first derivative of the Gaussian pulse generated by the transmitter. The response of the receive antenna to this ideal pulse is given by the second derivative Gaussian waveform,

$$s_{rec}(t) = \left[1 - 4\pi\left(\frac{t-t_d}{\tau_m}\right)^2\right] \exp\left[-2\pi\left(\frac{t-t_d}{\tau_m}\right)^2\right], \tag{1}$$

where $t_d$ represents the location of the pulse center in time and $\tau_m$ is a parameter which determines the temporal width of the pulse, and is approximately 0.8 ns in this work.

*This work was supported in part by the Integrated Media Systems Center at the University of Southern California, in part by the Joint Services Electronics Program under contract F49620-94-022 and in part by TRW Space and Electronics Group.



0-7803-4478-2/98/$10.00 (c) 1998 IEEE

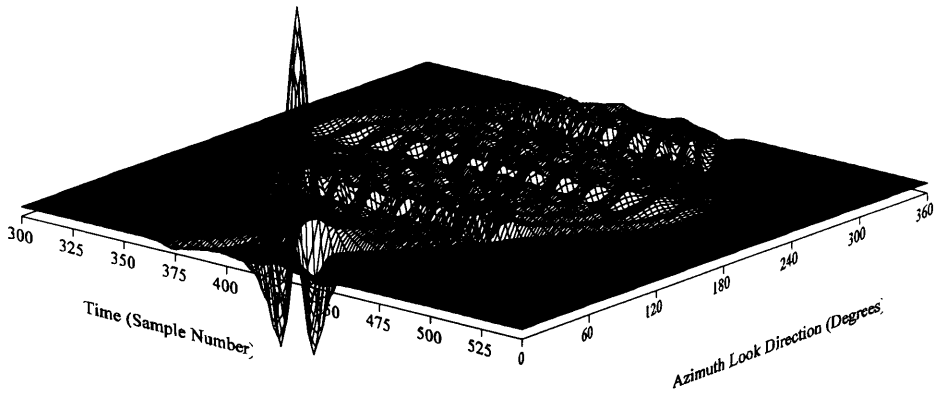


Figure 1: Beamformer response vs. time and azimuth look angle at $90^o$ elevation, for the 49 element planar array with $s_{rec}(t)$ incident at an azimuth angle of $45^o$ and $90^o$ elevation.

### B. UWB Propagation Experiment

An ultra-wide bandwidth (UWB) signal propagation experiment was performed in an office building to evaluate the UWB signal propagation channel [1]. Signal propagation measurements were made from a fixed impulse transmitter location to 14 different rooms and hallways of the office building, transmitting a pulse train of duty cycle 0.2% and of period of 500 nanoseconds. In each room, measurements over a window of 300 nanoseconds were made at 49 different locations arranged spatially in a fixed-height, 7 sensor $\times$ 7 sensor square grid with 6 inch inter-sensor spacing. The same absolute delay reference for all recorded profiles was used.

## II. Beamforming with Ultra-Wideband Signals.

Given the bandwidth extent of the UWB signals, a delay-and-sum beamformer is used to process the received array of signals. Let the beamformer output for a planar array of sensors steered to an azimuth angle of $\theta$ and an elevation angle of $\phi$, on incidence of a plane wave from an azimuth angle of $\theta_o$ and an elevation angle of $\phi_o$, be represented by [4],

$$B(\theta,\phi,t) = \sum_{m,n} a_{m,n}(\theta,\phi)\, s_{rec}\left(t - (M-m)\frac{d_x}{c}(u-u_o) - (n-N)\frac{d_y}{c}(v-v_o)\right) \tag{2}$$

where $u = \sin\theta\sin\phi$, $v = \cos\theta\sin\phi$, $u_o = \sin\theta_o\sin\phi_o$, $v_o = \cos\theta_o\sin\phi_o$, $d_x$ and $d_y$ represent the inter-element spacings in the x and y-directions, respectively, and $a_{m,n}(\theta,\phi)$ is the antenna pattern of the element at position $(md_x, nd_y)$ in the array. All time-shifts are referenced to the array geometric center at $(Md_x, Nd_y)$. It is assumed here that each element has an isotropic pattern. Just as the expression for the array factor in the narrowband case is dependent on the assumed sinusoidal signal characteristics, this expression also explicitly depends on the received pulse shape. From (2) it is seen that the beamformer can impart distortions to the received signal as it is steered away from the actual angle-of-arrival.

The response of the measurement array to $s_{rec}(t)$ is shown in Figure 1. The beamformer was applied to measured data, and one case containing a pulse with arrival angle similar to that in Figure 1 is shown in Figure 2. Other signal components are present in this case, but not easily distinguishable.

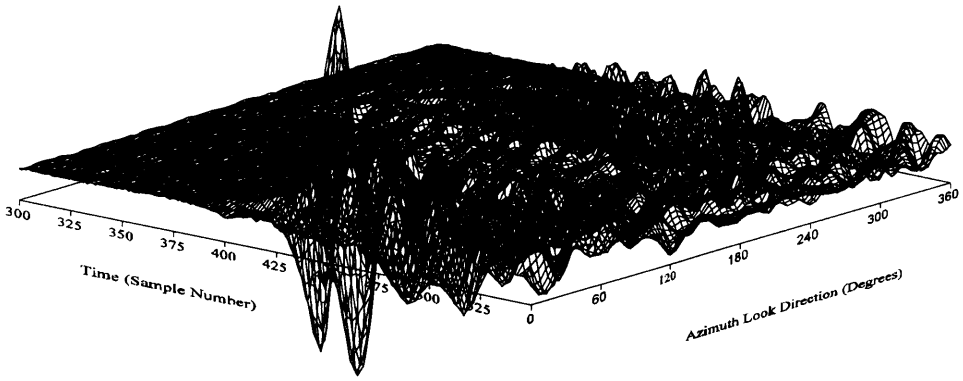


Figure 2: Beamformer response to measured data for a high SNR case at $90^o$ elevation.

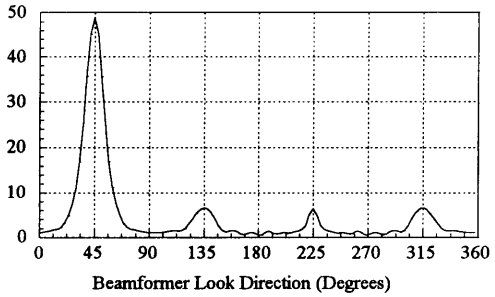


Figure 3: Maximum projection for 49 element planar beamformer on incidence from 45 degrees.

Another plot of the beamformer output, where the time dependence has been removed, and the maximum amplitude at each look direction is recorded, is given in Figure 3 for the beamformer output of Figure 1. UWB array performance is governed by the ability to resolve closely spaced sources and the sidelobe level of the beamformer. Accepting the resolution of the array, sidelobes with amplitude of nearly 1/7 that of the main beam appear in Figure 3. The dynamic range of this beamformer in the absence of any post-processing is therefore limited by these sidelobes to approximately $20\log_{10}(7/1)$ or 16.9 dB.

## III. Channel Characterization.

The goal of a channel characterization in this context is to extract the structure of the channel from the received data. Define the channel model for impulse radio communications to be

$$r(t) = \sum_{k=1}^{N} A_k s_{rec,k}(t - \tau_k, \theta_k, \phi_k) + n(t) \tag{3}$$

where $\tau_k$ is the time-of-arrival of the $k^{th}$ out of N components, at an azimuth angle of $\theta_k$ degrees and an elevation angle of $\phi_k$ degrees. The received impulse waveform, $s_{rec,k}(t)$ depends on the index $k$, due to variations in the received signal shape. This dictates that the algorithm should estimate $s_{rec,k}(t)$ from the

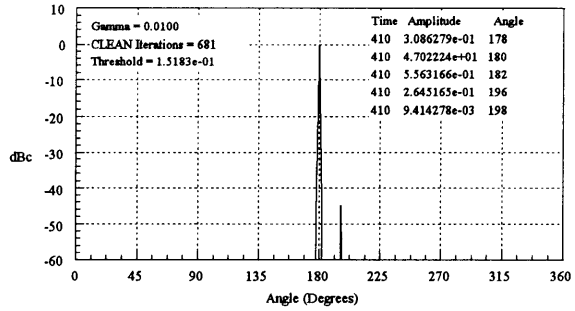


Figure 4: CLEAN beam for two signals with a 40dB difference in signal level.

received data. The technique proposed here for evaluation of the UWB channel is the CLEAN algorithm, introduced in [7] for the enhancement of radio astronomical maps of the sky. The algorithm has also found utility in the microwave and radar imaging communities [5], [8], for the reduction of antenna sidelobes. Use of the CLEAN algorithm here involves a variable array response with extent both in time and space. Modifications were therefore made, allowing estimation of the array response from the beamformer output. The steps in this modified CLEAN algorithm are as follows:

1. Generate the beamformer response to the input data over a window in time and angle.
2. Search the beamformer output window over time and angle for the peak response.
3. Determine and store the amplitude and the time and angle-of-arrival of this peak response.
4. Estimate the peak signal from the beamformer response and store this waveform.
5. Generate the beamformer response to this estimated waveform.
6. Update the beamformer response by subtracting a fraction $\gamma$ of the response to the estimated signal from the previous beamformer response,

$$B_n(\theta,t) = B_{n-1}(\theta,t) - \gamma \hat{B}_{k,n-1}(\theta,t) \tag{4}$$

where,
$k$ is an index of the largest response in $B_{n-1}(\theta,t)$.
$B_n(\theta,t)$ is the beamformer response at the $n^{th}$ iteration.
$\hat{B}_{k,n-1}(\theta,t)$ is the estimated beamformer response to the $k^{th}$ impulse at time $n-1$.

7. Add the current signal amplitude, scaled by $\gamma$, to the appropriate place in a list of signal locations.
8. If a stopping criterion (a threshold on the signal level or residual energy) is not met, go to step 2.
9. Generate a list of the signals found, including amplitude and the time and angle-of-arrival.
10. Form the CLEAN map by convolving the list of signals with delta functions.

CLEAN has been characterized using simulated impulse radio waveforms to define its performance limits. The ability to identify co-incident impulses separated by the array angular resolution limit, both for equi-amplitude signals and those with an amplitude difference of 40 dB, was demonstrated. This is a significant improvement in the dynamic range, and the output of the algorithm is shown in Figure 4 for $2^o$ of angular quantization. Note that the ability of the algorithm to resolve closely spaced sources is a function of both the angular and temporal separation of the sources. The performance of the algorithm was also tested in the

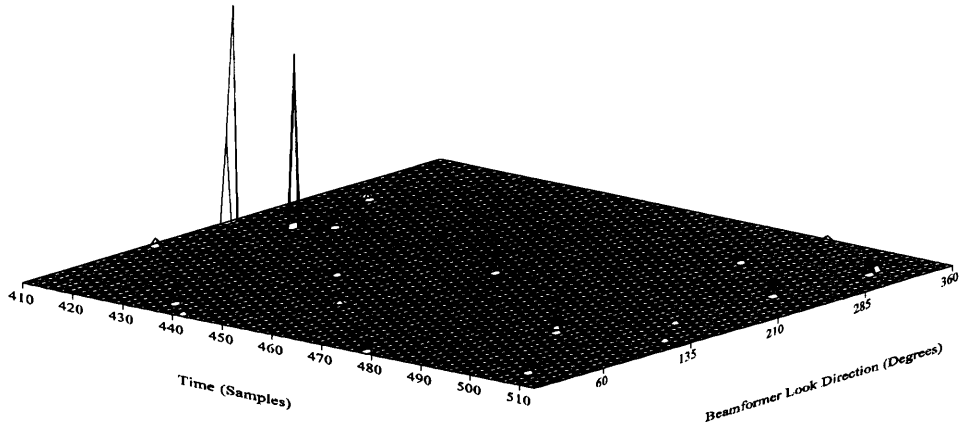


Figure 5: CLEAN map for two signals in noise.

presence of noise, on input of two impulses separated in time by 0.5 ns and in azimuth angle by $10^o$. A typical CLEAN map for a moderate SNR is shown in Figure 5.

Current work includes the development of a theory for the selection of the loop gain and stopping criterion. Efficient methods of accounting for wavefront curvature and sensor position errors are also under investigation, as are improved array geometries for future measurements.

## IV. Acknowledgments.

The assistance and cooperation of Time-Domain Systems, in making the measurements referred to in this paper, and the Integrated Media Systems Center (IMSC) at the University of Southern California is acknowledged.

## References

[1] R. A. Scholtz and M.Z. Win, "Impulse Radio", *Personal Indoor Mobile Radio Conference*, Helsinki, Finland, Sept. 1997, Printed in *Wireless Communications: TDMA vs. CDMA*, S.G. Glisic and P.A. Leppänen, eds., Kluwer Academic Publishers, 1997.

[2] R.A. Scholtz, "Multiple Access with Time-Hopping Impulse Modulation," in *Proc. Milcom*, Oct. 1993.

[3] M.Z. Win, R.A. Scholtz, M.A. Barnes, "Ultra-Wideband Signal Propagation for Indoor Wireless Communications", *Proc. IEEE Int. Conf. on Comm.*, June, 1997.

[4] J.D. Taylor, *Introduction to Ultra-Wideband Radar Systems*, CRC Press, Boca Raton, FL, 1995

[5] J. Tsao and B.D. Steinberg, "Reduction of Sidelobe and Speckle Artifacts in Microwave Imaging: The CLEAN Technique", *IEEE Trans. on Antennas and Prop.*, vol. 36, No. 4, April, 1988.

[6] OSD/DARPA, *Ultra-Wideband Radar Review Panel, Assessment of Ultra-Wideband (UWB) Technology*, DARPA, Arlington, VA, 1990.

[7] J.A. Högbom, "Aperture Synthesis with a Non-Regular Distribution of Interferometer Baselines", *Astron. and Astrophys. Suppl. Ser.*, vol. 15, p.417-426, 1974.

[8] Q. Spencer, M. Rice, B. Jeffs, M. Jensen, "Indoor Wideband Time/Angle of Arrival Multipath Propagation Results", *IEEE Vehicular Technology Conference*, IEEE, 1997, p. 1410-1414.